# Anode design modeling for improved energy efficiency

**Ayoola Brimmo[1], Mohamed Mahmoud[2], Khalil Khaji[3], Mohamed I Hassan[4]**

1. Research Engineer,
4. Assistant Professor,
Mechanical and Materials Engineering Department, Masdar Institute of Science and Technology Abu Dhabi, UAE
2. Manager, Technology Improvements, Technology Development & Transfer
3. Manager, Process Control & Improvement, Carbon & Port
Emirates Global Aluminium (EGA) Al Taweelah (EMAL)
Corresponding author: miali@masdar.ac.ae

**Abstract**

In aluminum reduction technology, a substantial portion of the anode's voltage drop is a consequence of imperfect contact between the cast iron thimble (connector) and the anode's carbon block. A useful tool for optimising these contacts, in order to improve the anode's energy efficiency, is the electro-thermo-mechanical (ETM) mathematical model. Using the ETM, this study elucidates on the underlying problem of voltage drop within the anode of an aluminum reduction cell and presents alleviation strategies. Adequate correlations for the temperature and pressure dependent electrical contact conductance (ECC) were utilised to facilitate realistic results. Two voltage drop mitigation approaches were considered: (i) metallurgical modifications of the steel stub for favorable thermal and mechanical properties; and (ii) geometrical modification of the thimble to maximise real-contact area. Results show that both strategies could reduce the electric contact resistance and hence, reduce the overall anode voltage drop. Strong dependence of the results on the Contact Stiffness Factor (CSF) suggests the need for further calibration with onsite measurements for quantitatively accurate results. Also, as our model is based on fresh anodes, conclusions cannot be drawn about the efficacy of our strategies in saving energy as the anode life approaches its end. Overall, this article documents our experience in developing ETM models of the anode.

**Keywords:** Aluminum reduction; anode voltage drop; electrical contact resistance.

## 1 Introduction

The anode assembly of the aluminum reduction cell is usually coupled by connecting steel stubs to a carbon block using a molten cast iron thimble. However, as cast iron shrinks during solidification and cast iron does not wet carbon, a gap arises between the thimble and the carbon block. This imperfect contact contributes to the voltage drop of the cell during operations, which could cost a typical smelter up to USD 2.2 million per annum. This is a magnitude that legitimately necessitates concern. Taking a deeper probe at this problem, the origin of the voltage drop can be traced to the presence of asperities on real surfaces when contact is attempted; only localized metallic contacts are made and these act as the conducting path for the transfer of electrical current [1]. A combination of these conducting sites across the contact surface forms the "real-contact area", which is the major parameter to enhance in order to minimise voltage drop at the contact interface [1, 2].

Experimental studies focused on mitigating this voltage drop can be traced back to the 1970s [3, 4]. The most imperative findings from early studies were relationships between the electrical contact resistances and the thermo-mechanical loading experienced at the contact [3, 4, 5, 6]. In these studies, dependence of the electric contact resistance on the contact's thermodynamic conditions is unequivocally reported. More recent experimental studies in this line have corroborated earlier findings [7, 8] and attempted to deduce equations which describe the electric contact resistance as a function of contact temperature and pressure [9, 10, 11]. However, the high cost of these experiments, coupled with the repetitive nature of optimisation studies, precluded the development of voltage drop mitigation strategies using this approach.

Mathematical modelling, which has experienced significant growth in the past two decades, has also gained huge attention in the aluminum research and development community. Consequently, efforts in mitigating anode voltage drop have been extended to computational models. The electro-thermal (ET) models of the anode developed in the 1990s [12, 13] pioneered such works, but omission of a mechanical model in Dupuis [13] and Hou et al [12] limited the robustness of their analyses. Richard et al's electro-thermo-mechanical (ETM) coupling [14] presented a more rigorous approach. Aside from incorporating the pressure and temperature dependent electric contact resistance, Richard et al's study [14] established a technique for estimating the initial separation between carbon and cast iron at ambient temperature. This technique is now widely applied in developing finite element models [15]. Richard et al [14] showed that increasing the effective cast iron mass (either by lengthening the flutes or by adding more of them) results in a reduced voltage drop until a minimum is achieved. Beyond this value, adding more cast iron led to a rapid deterioration of the anode's energy efficiency. An alternate study revealed that, despite the increased nominal surface area and mass of the thimble, the resulting anode voltage drop was found to increase slightly due to the decrease of contact quality [16]. This finding correlates with other studies, which showed that an increment in the thimble surface area does not guarantee a reduction in contact voltage drop [17, 16]. This suggests that the relation between the temperature, pressure and, the real-contact area variables is highly non-linear. Undoubtedly, the complexity of deciphering the relation between the contact's thermodynamic conditions and its real-contact area has greatly hampered progress in this field. Till date, a general conclusion on stub-hole design has not been made – no real solution has been proposed, with the majority of the modeling studies being stopped at portraying the prospect of the finite element analysis (FEA) tool [10, 17, 14, 16].

In maximising the real-contact surface area and pressure, a closer look has to be taken into the macroscopic structural deformation of the anode stub. Fortin et al [18] demonstrated how the typical tripod (yoke) configuration of the steel stub has a significant effect on its thermo-mechanical deformation. As shown in Figure 1, due to the thermal-expansion in the horizontal direction, with the stubs immobile at the bottom, the outer stubs tilt to generate a pressure bias on the carbon block to create a phenomenon known as the "toe-in" effect. This generates an unsymmetrical contact area and pressure which have distributions that are further complicated by the transfer of the anode assembly's weight to the flutes due to the "hanging" of the anode set-up from the cell's superstructure.

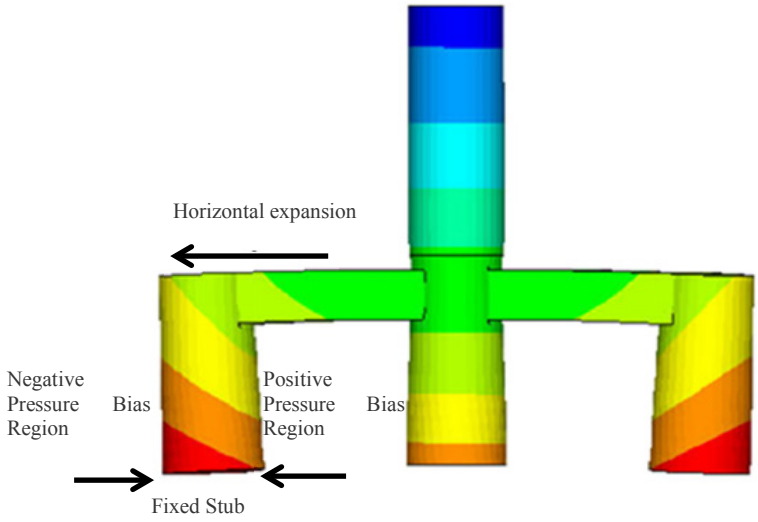


**Figure 1. Toe in effect of the tripod (yoke) steel stub configuration (magnified by 30) [18].**

Very little can be done to improve the real-contact area at the negatively-biased pressure region. Hence, in mitigating the contact voltage drop for the tripod configuration stub, efforts should be focused on maximising the contact pressure at the positively-biased pressure region. This

requires an unsymmetrical geometric modification approach, as opposed to the symmetrical solutions previously proposed [14, 15, 16]

In this study, we attempted to maximise the contact pressure and real-contact area at the positively-biased pressure region by maximising the thimble and stub conductance with the carbon block (i) geometrically (through thimble design) and (ii) metallurgically (through stub thermal-expansion). From a geometrical perspective, modifications were made to the thimble in order to redistribute its surface area and orient its flutes to favour the positively-biased region. Also, the steel stub material was replaced with a grade of steel which has a thermal expansion modified to exert an amount of pressure on the thimble enough to close the thimble-carbon gap. The effect of both approaches on the contact voltage drop was investigated using the developed ETM Finite Element Models (FEM) of the anode assembly. In developing the models with techniques validated in our previous work [11], various contact element parameters and boundary conditions were considered. The effect of these variables on the model's estimate of the contact voltage drop was also demonstrated.

## 2. Mathematical Modeling

The computational domain and boundary conditions of the anode assembly model, developed on the ANSYS Mechanical platform, are presented in Figure 2. It is important to note that this anode set-up is based on the dimensions of the beginning-of-life anode. The electric current applied is based on that of a high amperage aluminum smelting cell [19]. Based on the operating bath temperature of a typical cell, a temperature of 960 ˚C was applied at the bottom surface of the carbon block which is usually immersed into the bath. Convection heat transfer coefficients and temperatures were based on the suggestions by Fortin et al [15] and thermal measurements made at a smelter. It is important to note that although the anode cover wais not explicitly included in the model, the effect it has on insulating the top of the carbon block and stubs were taken into account using an adiabatic boundary condition. The top of the stub was constrained in order to simulate the actual operation of the anode where it is hung from the superstructure. A force of 3.34 kN was applied at the bottom of the anode block to take into account the buoyancy force exerted by the bath, based on the immersed volume of the fresh anode. The material properties of the anode assembly were obtained from the following references [7, 8, 20].

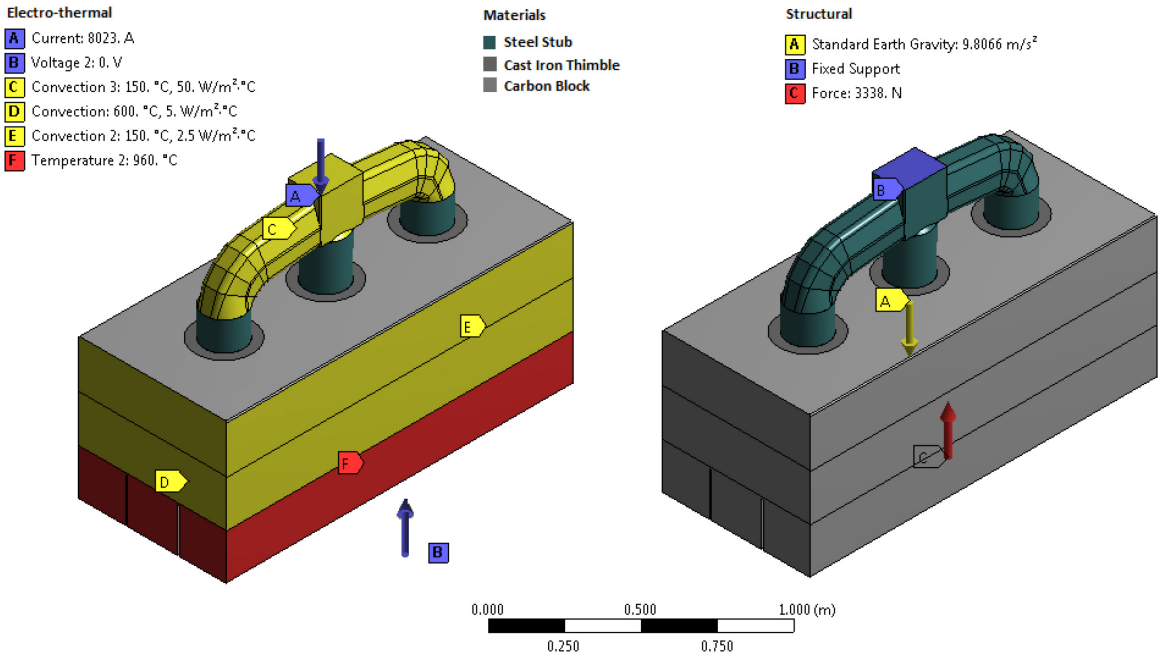


**Figure 2. Computational model and boundary conditions.**

SOLID227 elements – 3D, 10 node element with temperature, structural and voltage degrees of freedom – were used to perform the ETM coupling required for the analyses. In performing this coupling, two approaches were considered (1) single run coupling of the ETM calculation and; (2) a manual solution transfer between ET and thermo-mechanical models. Using the single run technique, the physics of coupling was accounted for mathematically by the multiplication of off-diagonal sub matrices with the single column matrix containing the degrees of freedom (DOF) – strong or simultaneous coupling of all DOF [21]. The advantage of this solver is the ease with which the whole run can be solved with a single bypass and no manual effort. However, having three DOF significantly increases the size of the problem and causes a matrix reformulation problem – for each reformulation of a section of the matrix associated with one degree of freedom, the whole matrix is reformed. As such, convergence could be very tedious to attain, especially with the unstable nature of the thimble-carbon contacts being modelled. On the other hand, the manual solution transfer technique involves a manual back and forth transfer of the results between an ET and a thermo-mechanical model. It is noteworthy that the individual ET and thermo-mechanical models are similarly strongly coupled however, with only two DOF each. Using this approach, the un-deformed geometry of the anode is fed into the ET model and the resulting temperature profile is used as a load in the thermo-mechanical model. Subsequently, the deformed geometry and contact pressure are calculated by the thermo-mechanical model and transferred back manually to the electro-thermal model until a convergence is attained. The disadvantage of this approach lies in its manual nature. However, it allows for better control of the model and its convergence. More details on this technique can be found in our previous work [11].

Connections between dissimilar bodies were handled using the CONTA174-TARGET170 contact elements, which also have the temperature, structural and electrical DOF. To ensure the Electric Contact Conductance (ECC) was modelled as a function of the contact's element temperature and pressure, correlations developed from Rhedey and Castonquay's [6, 11] measurements were utilised. The assignment of ECC at each contact node was automated to be updated, each iteration based on the nodal temperature, pressure and the inputted constitutive equation. In our previous study, the Contact Stiffness Factor (CSF), which is the proportionality constant of the relation between the contact pressure and contact gap size, based on the adapted Augmented Lagrangian model [22] shown in Equation (1), was found to best fit experimental measurements at a value of 0.1. However, as our previous model was not based on the tripod stub configuration, this value cannot be confidently adapted in this study for quantitatively accurate results. Hence a range of CSF between 0.1 and 1 was used to demonstrate the effect of this parameter on the modelled estimate of the contact voltage drop. The effect of using the "rough contact elements" as opposed to the friction contact elements (0.2 friction coefficient) was also demonstrated.

$$\begin{aligned} &if\ U > 0;\ P = 0 \\ &if\ U \le 0;\ P = kU + \Lambda_i \end{aligned} \tag{1}$$

Where $P$ is the contact pressure, $k$ is the contact stiffness, $U$ is the contact gap and $\Lambda_i$ is a function of the Lagrange multiplier.

The gap created by the shrinkage of the cast iron thimble is usually implemented in finite element models of the anode assembly [14, 18, 16] by introducing a few centimeters of "air gap" based on the linear equation suggested by Richard [23]. However, this equation predicts a uniform gap across the thimble surface area. The "toe-in" effect of the steel stub, as shown in Figure 1, shows that this approximation is inaccurate as the stub expansion exerts a non-uniform pressure and hence, creates a non-uniform gap across the contact surface. As such, in our model, we adapted a technique which involved specifying the cast iron reference temperature (stress free temperature) as its melting point of 1 400 °C – the temperature at which it is poured to fill the space between the stub and the carbon. As thermal strain is calculated based on this temperature, adequate gap values are computed by the code upon cooling, taking into consideration the toe-in phenomena.

The computational domain was discretised by linear tetrahedral elements; with a very high grid density at the contact interfaces. To ensure consistency, identical meshes were used for all models/sub-models. Due to the non-uniform voltage drop across the thimble-carbon interface, it is difficult to measure the exact voltage drop contribution of the imperfect contacts using probes. Hence, in order to isolate this portion of the voltage drop, a base case model with perfect "bonded" thimble-carbon contacts was run and the calculated overall anode voltage drop was subtracted from that calculated by models with contact elements which allow separation.

The typical thimble design is such that a number of rectangular shape flutes are symmetrically threaded into the carbon block as shown in Figure 3(a). In the present study, we proposed a "mushroom shape" flute to maximise the contact surface area perpendicular to the "toe-in" direction, as shown in Figure 3(b), and an inversion of one-half of the two end thimble flutes to favour the positively-biased pressure region, as shown in Figure 3(c).

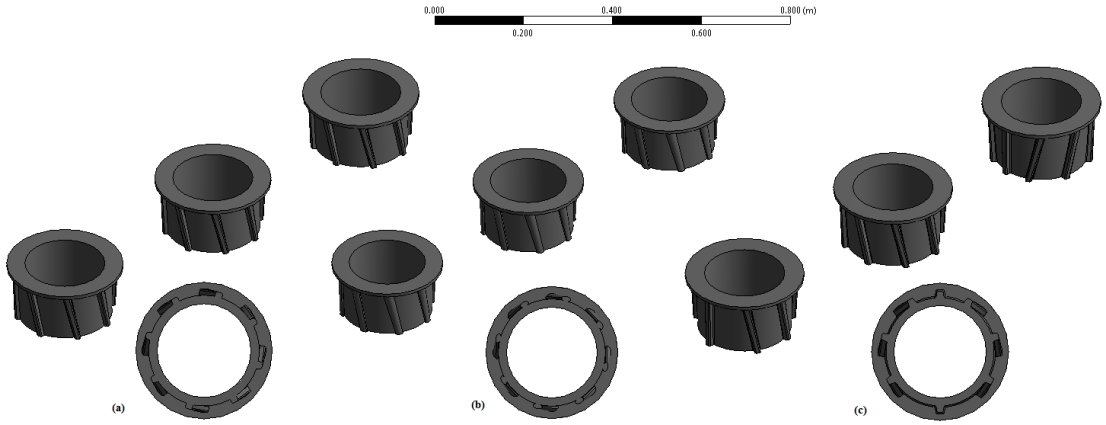


**Figure 3. Thimble configuration (a) typical design; (b) proposed mushroom shape; (c) inverted flutes.**

Based on the utilised anode dimensions, a steel material with a thermal expansion coefficient high enough to counter the average gap created by the thimble was designed, using fundamental metallurgical principles. Using such material as the anode stub, it was envisaged that the expansion of the steel material would exert enough pressure on the thimble to close the thimble-carbon block gap. Based on this premise, we replaced the model's stub with steel materials of varying thermal expansion coefficient (TEC) to investigate the effect on the model estimate of the contact voltage drop. Contact voltage drops were then compared using each of the modelled stub materials to evaluate the authenticity of our premise. It must be noted that the TEC inputs in the model were a function of temperature hence, these inputs were in the form of temperature dependent equations. The following section present results from our model calculations and discussions regarding the aforementioned contact voltage drop mitigation efforts.

## 3. Results

Only a 1 % deviation was recorded between the overall anode voltage drops calculated using the automated and manual approaches. Based on this, we conclude that both techniques arrive at the same results. As the manual iteration approach is in essence an interchangeably weak coupling between strongly coupled ET and thermo-mechanical models, this concurrence was expected. However, due to the complexity of the matrix involved with the contacts' non-linearity and the irregularity of the thimble geometry, convergence was very difficult to reach using a single run through the automated TEM coupling model. Hence, for the rest of our analysis, we adapted the manual technique which afforded full control of the whole modeling procedure.

Figure 4 shows contact pressure profiles and their corresponding ECC values. The contact regions with high pressure concentrations also have high ECC values. This trend is in accordance with our inputted constitutive equations. During the "toe-in" phenomena, the positively biased pressure regions are also the regions where the real-contact area is concentrated. It is expected that the electrons path would coincide with the positively biased pressure region; as such, this region was modelled with higher ECC values. The visual correlation between the contact pressure and ECC profiles, portrayed in Figure 4, validated the fitness of our ECC modeling approach.

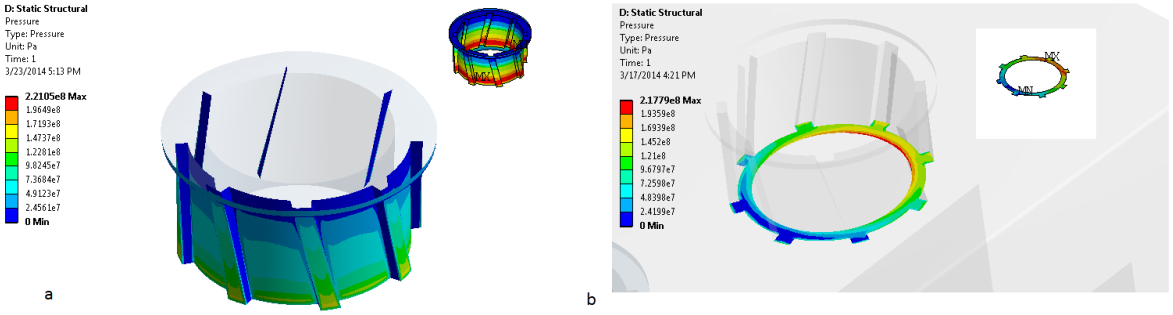


**Figure 4. Contact Pressure (inset mapped ECC) (a) Center thimble (b) right hand side thimble.**

Figure 5(a) shows the electric potential drop across the modelled anode assembly. It was observed that the yoke "toe-in" effect also creates a voltage drop bias at the outer end thimbles. In the region of high pressure, there is a concentration of the real-contact area and hence, lower voltage drop is experienced. Zooming into the left-hand side thimble (inset Figure 5(a)), the gaps generated at the negative pressure bias regions were visible. Also, a clearance was observed between the bottom surface of the stub and the carbon block. This was due to the hanging of the anode from the cell's superstructure. Hanging the assembly transfers the anode's weight to the flutes while the weight of the carbon block pulls it down to create the observed clearance. As such, there is no contact at the bottom of the stub and no electrical current is transferred to the carbon block via this path. Figure 5 (b) and (c) show the temperature and pressure profiles at the contact surfaces. Both profiles demonstrate the non-symmetric distribution of temperature and pressure, with biases being formed due to the "toe-in" effect. Also Figure 5 (c) shows that flutes, which are oriented in the direction of the stub tilt, have a higher pressure concentration than their adjacent counterpart. This suggests that orienting the flutes of the thimbles at the outer ends to be in line with the stub tilt might reduce the contact voltage drop. This was the design proposed in Figure 3 (c).

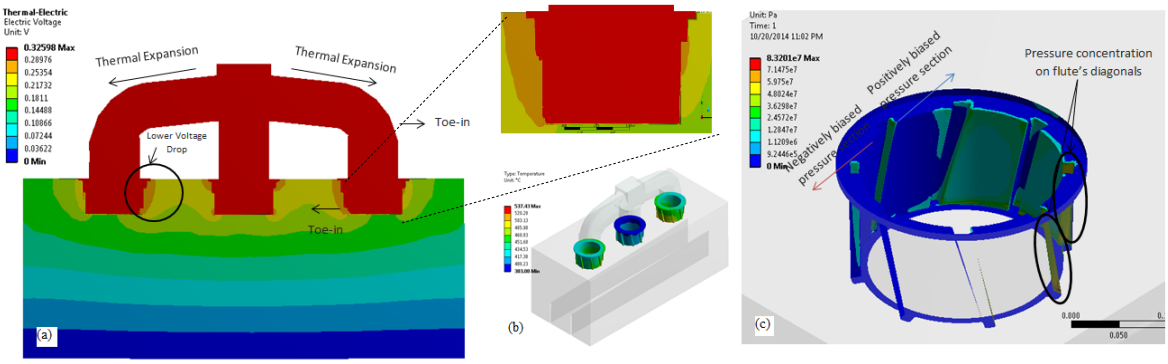


**Figure 5. Model-calculated (a) electrical potential; (b) temperature; (c) contact pressure distribution.**

Figure 6 show that the "rough contacts" underestimate the contact voltage drop, for all considered stub diameters. Although the deviations between the estimates of the friction and rough contact elements are not consequential, as the friction contact elements allow sliding by a user defined coefficient of friction, this comparison demonstrates the quantitative significance of neglecting sliding by using the "rough contact" elements.

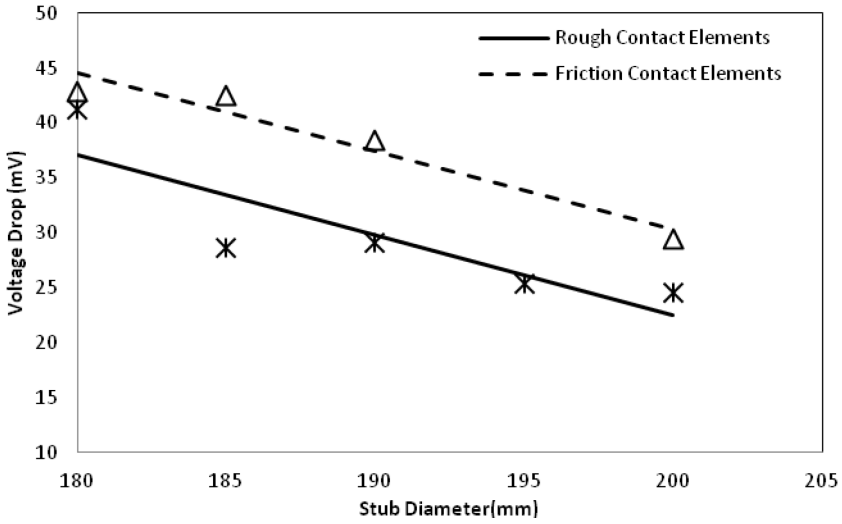


**Figure 6. Effect of varying type of contact elements.**

Figure 7 shows the contact voltage drop as a function of the thimble mass, design and location of the fixed constraint. The thimble mass was varied by adjusting the thimble depth and the stub's diameter. The contact voltage drop for each thimble mass was calculated with the fixed boundary condition either at the top of the stub, as shown in Figure 2, or at the bottom of the carbon block. This was used to demonstrate how a faulty boundary condition could yield misleading results with meaurable consequences. It is worthy to note that the results presented in Figure 7 were estimated using a CSF of 0.1. Generally, the contact voltage drops as the thimble mass increases. This was expected, as an increment of stub depth increases the real-contact area. However, increasing the thimble mass by reducing the stub diameter was not considered in this study because it would not have any effect on the thimble-carbon contact surface area, but would rather undesirably increase the thimble thickness. Increasing the thimble thickness would increase the thimble-carbon contact-resistance due to the excessive cast iron shrinkage that would be produced by the thicker cast iron.

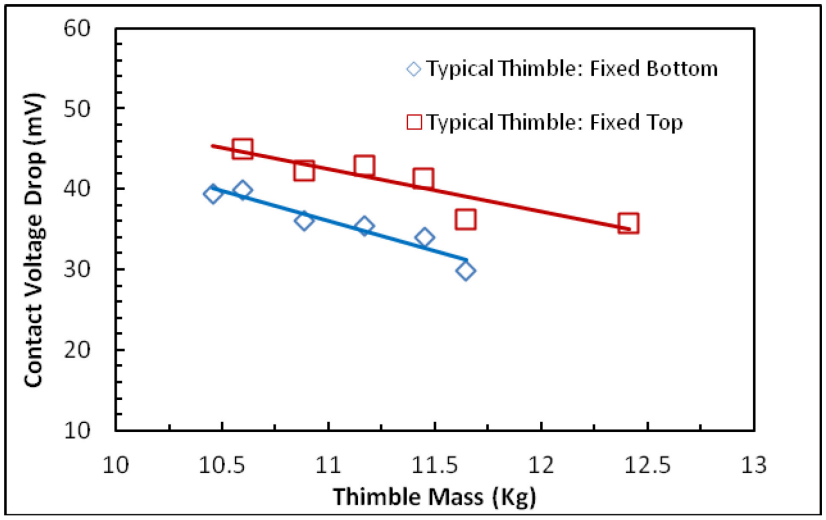


**Figure 7. Effect of fixed constraint location on thimble design consideration.**

This is portrayed in some data points in Figure 7 which show that an increase in the thimble mass does not necessarily guarantee a reduction in contact voltage drop in accordance with previous reports [14, 16, 17]. Furthermore, Figure 7 shows that models placing the Fixed Constraint at the bottom of the assembly produce a result which underestimates the contact voltage drop for a given thimble design. This trend can be attributed to the increased separation, especially at the bottom of the stub, which arises when the assembly is hung from the superstructure (modelled as Fixed Top). The mushroom-shaped flute design seems to result in a reduced voltage drop when the assembly is constrained from the bottom, but this is not the case when the anode is rightly hung from the superstructure. This is due to the improved radial surface area of the mushroom flutes. which has greater importance when the assembly is constrained at the bottom. When constrained at the top, the weight of the anode is supported by the flute sides. Therefore, reducing the flute thickness is not favourable for reducing the contact voltage drop. Figure 8 shows a comprehensive comparison of our modelling results for different thimble designs at the two examined CSF.

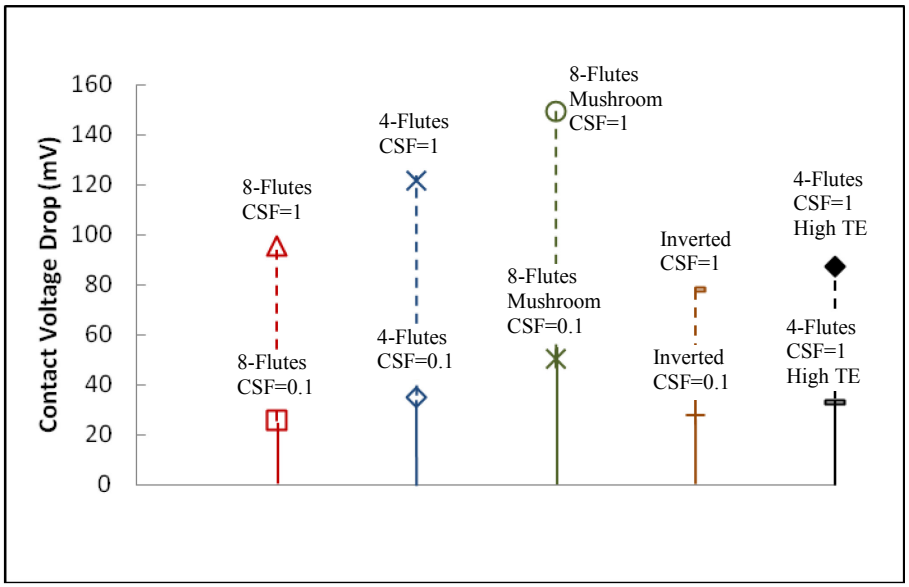


**Figure 8. Voltage drop comparison for modified thimble geometries.**

Figure 8 shows the effect of the thimble geometrical modification, at CSF values of 0.1 and 1, on the contact voltage drop. For all designs, the CSF of 1 result in a lower contact voltage drop than that of a CSF of 0.1.

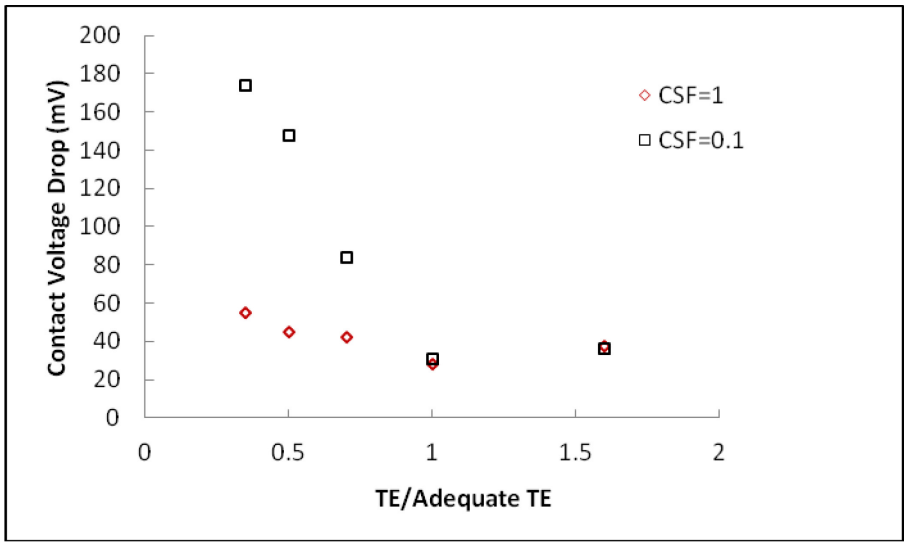

**Figure 9. Voltage drop comparison for modified steel stub metallurgy.**

As an increase in CSF signifies an increase in the stiffness of a hypothetical spring placed between the contacting surfaces, less separation and higher contact pressure are expected at higher CSF values. Although experimental calibration is required to calibrate the model accurately for an adequate CSF, based on previous experience in developing this type of model [11] and previous estimates of the contact voltage drop of the anode [17], the right CSF value is expected to fall between 0.1 and 1. Based on this premise, we ranked the designs presented in Figure 8 from lowest to highest contact voltage drop as: Typical Thimble (Inverted flutes), Typical Thimble (4 flutes, Inverted flutes), Typical Thimble, Typical Thimble (4 flutes), Mushroom Thimble. Apparently, as previously hypothesized, inversion of the flute direction reduces the contact voltage drop.

Figure 9 shows that increments in the stub material's TEC reduce the contact voltage drop until our estimated adequate TEC value is attained. As the thermal expansion coefficient of the steal stub is increased, the gap between the thimble and the carbon is reduced, hence reducing the contact voltage drop. However, when the gap is fully closed, further increments cause penetration of the thimble in the carbon, which is translated by our model as a negative contact gap. For simplicity, at gaps of 0 mm and below, the contact pressure is modelled as 0 Pa, hence penetration is not adequately taken into account. This is why the model portrays increments in contact voltage drop as the TEC value exceeds the "Adequate TEC". As no fracture mechanism was included in our model, we cannot tell if the thimble mechanical integrity was sustained at the increased pressure.

Although both strategies portray an improvement in energy efficiency, we cannot draw conclusions on the performance of these designs when used in an anode reaching its end-of-life. As the carbon block is consumed with anode age, the thermodynamic conditions at the thimble-carbon interface change, which alters the validity of the current model. Further studies are recommended to cover the life span of the anode in order to ensure that energy saving strategies are applicable through-out the anode life.

## 4. Conclusion

In this study, we present our developed TEM FEM for modelling the aluminum reduction cell's anode assembly. Using the TEM, we evaluate the fitness of two voltage drop reduction approaches: thimble design and stub steel thermal expansion. The effect of varying the model boundary conditions, CSF and thimble mass on the contact voltage drop were also highlighted. Results showed that there is room for reducing the contact voltage drop by changing the thimble flute design, but strong dependence of the results on the CSF and lack of a fracture mechanism in our models suggest the need for further calibration with experiments.

## 5. Acknowledgments

This project was sponsored by Emirates Global Aluminum (EGA). We would like to thank all the members of staff at the EGA Al Taweelah smelter who contributed their efforts and useful discussions. We would also like to acknowledge the fruitful discussions with the EGA Jebel Ali smelter team and for their very insightful comments regarding the operation and performance of their cells.

## 6. References

1. M. Braunovic, "Power connections," in Electrical Contacts, Boston, P. Slade and M. Dekker, 155, p. 1999.
2. R. Holm, Electric Contacts; Theory and Applications, New York: Springer, 1967.
3. R.W. Peterson, "Studies of stub to carbon voltage," *Light Metals,* 1978, pp 367-378.
4. W. Peterson, "Temperature and voltage measurements in Hall cell anodes," *Light Metals,* 1976, pp 365-382.

5. D.G. Brooks and V.L. Bullough, "Factors in the design of reduction cell anodes," *Light Metals ,* 1984, pp 961-976.
6. P.J. Rhedey and L. Castonguay, "Effects of carbonaceous rodding mix formulation on steel-carbon contact resistance," *Light Metals,* 1985, pp 1089-1105.
7. M. Sørlie and H. Gran, "Cathode collector bar-to-carbon contact resistance," *Light Metals,* 1992, pp 779-787.
8. S. Wilkening and J.Cote, "Problems of the Stub- Anode Connection," *Light Metals,* 2007, pp 534- 542.
9. D. Richard, M. Fafard, R. Lacroix, P.l Cle´ry and Y. Maltais, "Carbon to cast iron electrical contact resistance constitutive model for finite element analysis," *Journal of Materials Processing Technology,* vol. 132, 2003, pp 119-131.
10. D. Molenaar, K. Ding and A. Kapoor, "Development of industrial benchmark finite element analysis model to study energy efficient electrical connections for primary aluminium smelters," *Light Metals,* 2011, pp 959-990.
11. A.T. Brimmo and M.I. Hassan, "Modeling the Electrical Contact Resistance at Steel-Carbon Interfaces," *JOM,* 2015, pp xx-yy.
12. T.X. Hou, Q. Jiao, E. Chin, W. Crowell and C. Celik, "A numerical model for improving anode stub design in aluminum smelting process," *Light Metals,* 1995, pp 755-761 .
13. M. Dupuis, "Computation of aluminum reduction cell energy balance using Ansys finite element models," *Light Metals,* 1998, pp 409-417.
14. D. Richard, M. Fafard, R. Lacroix, P. CleHry and Y. Maltais, "Aluminum reduction cell anode stub hole design using weakly coupled thermo-electro-mechanical Finite element models," *Finite Elements in Analysis and Design,* vol. 37, 2001, pp 287-304 .
15. H. Fortin, M. Fafard, N. Kandev and P. Goulet, "FEM analysis of voltage drop in the anode connector assembly," *Light Metals,* 2009, pp 1055-1059.
16. D. Richard, P. Goulet, O. Trempe, M. Dupuis and M. Fafard, "Challenges in the stub hole optimization of cast iron rodded anodes," *Light Metals,* 2009, pp 1067-1072.
17. M. Dupuis, "Development and application of an Ansys® based thermo-electro-mechanical anode stub hole design tool," *Light Metals,* 2010, pp 433-438.
18. M. Reverdy, A. Zarouni, J. Faudou, Q. Galadari, S. A. A.A. Zarouni, K. Al-Aswad, M. Al-Jallaf, W. Al-Sayed and V. Potocnik, "Advancements of Dubal High Amperage Reduction Cell Technologies," Light Metals, 2013, pp 553-556.
19. F.P. Incopera, D.P. Dewitt, T.L. Bergman and A.S.Lavine, Fundamentals of Heat and Mass Transfer, Hoboken, New Jersey: John Wiley and Sons, 2007.
20. P. Kohnke, "Theory reference for Mechanical APDL and Mechanical Applications," ANSYS Inc, Canonsburg, PA, 2009.
21. J.C. Simo and T.A. Laursen, "An augmented Lagrangian treatment of contact problems involving friction," Computer and Structures, Vol. 42, No. 1, 1992, pp. 97-116.
22. D. Richard, Conception des tourillons d'anode en usage dans une cuve de Hall-Héroult à l'aide de la méthode des éléments finis, M.Sc. Thesis, 2000, Université Laval, Quebec, Canada.